Drivers and dynamics of Aedes albopictus expansion in 41 European countries: past reconstruction and future projections

Charlotte Perlant, Amandine Véber, Juliette Paireau, Cécile Tran-Kiem, U G Kraemer, Paolo Bosetti, Simon Cauchemez

Drivers and dynamics of *Aedes albopictus* expansion in 41 European countries: past reconstruction and future projections.

Charlotte Perlant[1],PhD, Amandine Véber[2], PhD, Juliette Paireau[1,3], PhD, Cécile Tran-Kiem[4], PhD, Moritz U.G. Kraemer[5,6], Pr, Paolo Bosetti[1*] PhD, and Simon Cauchemez [1*]Pr.

1. Mathematical Modelling of Infectious Diseases Unit, Institut Pasteur, Université de Paris Cité, INSERM U1332,CNRS UMR2000, Paris, France
2. Université Paris Cité, CNRS, MAP5, F-75006 Paris, France
3. Direction des Maladies Infectieuses, Santé publique France, Saint-Maurice, France
4. Vaccine and Infectious Disease Division, Fred Hutchinson Cancer Center, Seattle, USA
5. Department of Biology, University of Oxford, United Kingdom
6. Pandemic Sciences Institute, University of Oxford, United Kingdom

Corresponding author: Simon Cauchemez simon.cauchemez@pasteur.fr
*equally contributed

Keywords:
Competing interests statement: The authors declare no competing interest.

Abstract

Background

Aedes albopictus is a highly invasive mosquito and a competent vector of dengue, chikungunya, and Zika viruses. Since its introduction into Europe in 1979, it has expanded across large parts of the continent, increasing the risk of arboviral transmission. Its spread is driven by the interplay of human mobility, trade, and climatic conditions that are increasingly favorable to its establishment and persistence. However, these drivers are often modelled separately, limiting coherent uncertainty propagation.

Methods

We developed a unified mathematical model that jointly infers human-mediated introductions, dispersal, and biologically grounded climatic suitability from three decades of invasion data across over 1200 European spatial units. Unlike previous approaches that treat these processes independently, our model integrates them simultaneously, enabling consistent uncertainty propagation and projections under multiple greenhouse gas emission scenarios.

Findings

Median and minimum temperatures, relative humidity, solar radiation, and precipitation emerge as key climatic determinants, while long-range mobility, short-range diffusion, and national borders structure spatial spread. Projections indicate that the proportion of the European population exposed to *Aedes albopictus* could rise from 49% today to over 90% by 2049 under multiple climate scenarios. Country-level analyses identify four distinct risk trajectories of *Aedes albopictus* presence: already fully at risk, with increasing risk, persistently low-risk, and currently uninvaded but projected to face rising risk.

Interpretation

The identification of different national risk trajectories provide actionable guidance for surveillance, vector control, and public health preparedness. This framework delivers openly accessible projections of *Aedes albopictus* presence which provide a basis for future studies assessing potential arboviral risk under multiple climate scenarios.

Funding
DURABLE, IBEID, INCEPTION, LEAPS.

Research in context

Evidence before this study
We searched PubMed using the terms (Aedes albopictus) AND (Europe OR European) AND (expansion OR spread OR dispersal) AND (climate OR climatic OR environment) AND (model OR modeling) for studies published from data inception to February 17, 2026. We included all research articles in all languages.

To date, modeling studies of *Aedes albopictus* expansion in Europe have primarily focused on estimating climatic and environmental suitability using correlative species distribution or ecological niche models. These approaches identify areas environmentally compatible with establishment and project potential future range shifts under climate change scenarios. Other studies have adopted mechanistic or process-based models that explicitly represent mosquito life-cycle dynamics and temperature-dependent development, offering detailed biological realism, although often restricted to regional or local scales. Few studies have incorporated human-mediated dispersal, acknowledging the importance of transportation networks and introduction pressure in shaping invasion dynamics.

While these approaches have deepened our understanding of vector expansion, most frameworks consider climatic suitability, biological constraints, and introduction processes separately or sequentially. Integrating these drivers within a single mathematical structure remains methodologically challenging at continental scale and therefore limited.

Added value of this study
We developed a spatially explicit invasion model that jointly integrates human-mediated introduction pressure and climatic suitability shaped by mosquito biological characteristics within a single unified likelihood across more than 1,200 European spatial units over three decades. By integrating these processes simultaneously, our approach ensures coherent uncertainty propagation and maintains mechanistic interpretability when extrapolating to novel climatic conditions.

Our model reconstructs past expansion with high predictive accuracy and quantifies the relative contributions of gravity-based human mobility, short-range spatial diffusion, national borders, and five biologically grounded climatic variables. Beyond historical reconstruction, we project expansion under three contrasting greenhouse gas emission scenarios over the next 25 years. We estimate that the proportion of the European population living in areas where *Aedes albopictus* is present could increase from approximately 49% today to more than 90% by 2049. Our framework also classifies countries into four distinct risk trajectories, generating openly accessible projections directly usable for surveillance planning and public health preparedness.

Implications of all the available evidence

Arboviral outbreaks often follow mosquito establishment within a decade. By identifying areas where invasion is imminent, our results highlight critical windows for intensified surveillance and targeted vector control. Quantifying future expansion and population exposure over the next 25 years provides directly actionable information for anticipatory planning of dengue, chikungunya, and Zika prevention in Europe. Integrating mobility, biology, and climate this unified framework offers a realistic basis for preparedness strategies in a warming and increasingly connected continent.

Introduction

Vector-borne diseases represent a growing threat to global public health, with more than four billion people currently living in areas at risk (1). Among the vectors driving this expansion, *Aedes albopictus* stands out as one of the most invasive mosquito species worldwide (2) and a competent vector for major arboviruses, including dengue, chikungunya, and Zika (3–8). Originally native to Southeast Asia, *Aedes albopictus* has colonized all continents except Antarctica (9) and is now firmly established across large parts of Europe, where recent and recurrent dengue and chikungunya reported cases underscore its growing public health importance (10,11).

The rapid global expansion of *Aedes albopictus* is directly linked to globalization (12). International travel and trade have facilitated repeated introductions into new regions, notably through container habitats for the aquatic stages such as used tires and potted plants (13–15). These pathways are reinforced by the species' remarkable ecological and physiological plasticity. *Aedes albopictus* has adapted from primarily zoophilic to anthropophilic behavior (16,17), and exploits artificial containers in domestic and urban environments. Crucially, its desiccation-resistant eggs (18) and capacity for photoperiod-induced diapause (19) allow survival during transport and overwintering in temperate climates (20,21), enabling establishment far beyond its native range.

In Europe, *Aedes albopictus* was first introduced in the late 1970s in Albania (22), followed by subsequent establishments in Italy and a rapid expansion across the continent, especially the Mediterranean countries (23,24). Since then, the expansion of *Aedes albopictus* has accelerated, driven by the combined influence of climatic suitability, urbanization,

socioeconomic factors, and human mobility (25,26). Ongoing climate change (23) is expected to further facilitate northward expansion by transforming currently unsuitable areas into climatically suitable environments for mosquito survival and reproduction, increasing the likelihood of establishment and persistence in regions previously considered unsuitable. However, climatic suitability alone is not sufficient to explain observed invasion patterns, as establishment requires repeated introductions into suitable areas. International travel and trade therefore play a critical role by shaping where and when *Aedes albopictus* is introduced, directly conditioning whether climatically suitable regions are actually colonized. At the same time, the growing presence of competent vectors in Europe increases the risk that imported arboviruses lead to local transmission.

Despite extensive modeling efforts, the relative contribution of environmental suitability, mosquito biology and human-mediated introduction processes to successful colonization remains incompletely understood. Correlative niche models identify statistical associations between mosquito presence and climatic variables but typically ignore dispersal, introduction pressures and biological characteristics (27,28). As a result, they may overestimate risk in areas that are suitable but rarely exposed to introductions, and underestimate risk in marginal environments subject to frequent introductions. In contrast, mechanistic or process-based models describe the mosquito life cycle and movements but are often restricted to local scales (29–36) and do not capture large-scale heterogeneity in climate and human mobility. At the European scale, only a few studies have explicitly integrated climatic suitability with explicit introduction, spread processes and mosquito's biology within a unified framework (37,38). However, existing unified frameworks integrate these processes only partially or sequentially, conditioning invasion dynamics on pre-trained suitability maps or independently fitted life-cycle variables within multi-stage approaches. Their application to large-scale projections of future species expansion has remained limited.

Here, we develop a spatially explicit invasion model to assess the year-to-year colonization potential of *Aedes albopictus* across Europe, conditional on its current distribution. The model jointly integrates human-mediated introduction pressure and climatic suitability shaped by mosquito biological characteristics within a single framework. Using harmonized surveillance and environmental data, we reconstruct the historical spread, project future distributions under multiple climate change scenarios and time horizons, using several realizations per scenario to capture climatic uncertainty, and quantify how alternative climatic pathways may shape the future distribution of *Aedes albopictus*. Beyond reconstruction and projections, the framework allows classification of geographic regions into four distinct types of projected regional trajectories, reflecting variation in potential population exposure over time. By integrating the main ecological, biological, and human-related drivers of invasion without requiring computationally intensive multi-stage simulations, the approach provides an efficient tool for anticipating the future spread of *Aedes albopictus* in Europe. It is readily transferable to other regions or spatial scales, and generates openly accessible projections for the scientific community.

Material and Methods

Mosquito spatial spread data

We assembled a dataset describing the spatial spread and occurrence of *Aedes albopictus* in Europe from 1992 to 2024. Data for the period 1992–2017 were sourced from (27), which synthesizes published reports and expert surveillance data, and were extended up to 2024 using records from (39), coordinated by the European Centre for Disease Prevention and Control (ECDC) and the European Food Safety Authority (EFSA) (65).

Occurrence was aggregated to harmonised subnational administrative units using NUTS classifications for EU countries and GAUL classifications elsewhere. To ensure comparability across countries, spatial resolution was adjusted where necessary to reduce heterogeneity in unit area (appendix pp 3-6). Each unit was considered invaded from the first detection of any mosquito stage (introduced or established) and remained classified as invaded until the end of the study period. Prior to this first detection, the unit was considered uninvaded. In rare cases (<1% of observations), a recorded presence was followed by a verified absence. In these instances, the presence records were discarded, and the unit was considered uninvaded throughout the study period (appendix pp 3-6).

Human population sizes dataset

Annual population counts (1992-2024) were compiled from gridded population datasets extracted from SEDAC (40) (1992-2000), WorldPop (41) (2001-2020) and Eurostat (42) (2021-2024) and aggregated to administrative units using a consistent spatial framework. Missing recent values (2021-2024) were extrapolated by applying the median annual growth rate calculated over the period 1992–2020 to each affected unit (appendix p 13).

Future projections (2025-2049) were derived from gridded SSP-based datasets (43) aggregated to the same units. Continuity between historical data (up to 2024) and projections (2025–2049) was ensured by computing annual growth rates from the projected series and applying them to historical population sizes (appendix p 8).

Environmental data

Environmental covariates were selected from the variables routinely available in climate monitoring data to reflect key physiological and ecological constraints governing mosquito survival and development (66–72). The choice of variables was informed by experimental laboratory studies. Historical climate variables (1992-2024) were derived from ERA5 monthly land reanalysis data (44) and spatially aggregated to administrative units. Annual covariates include (appendix pp 14-18**,** appendix p 7):

- minimum temperature (*minT*), in Kelvin (K), representing lower thermal thresholds associated with overwintering survival,
- median dry-season (April-October) air temperature (*medT*), in Kelvin (K), capturing the optimal thermal range for mosquito survival and development,
- median dry-season relative humidity (*medRh*), expressed as a percentage, reflecting atmospheric moisture conditions associated with the presence of aquatic breeding habitats and egg viability,
- median dry-season solar radiation (*medSol*), in megajoules per square meter ($MJ.m^{-2}$), used as a proxy for photoperiodic conditions influencing egg hatching,
- total dry-season precipitation (*TotPrec*), in millimetres (mm), representing water availability for larval habitats and oviposition sites, jointly with relative humidity.

Climate projections (2025–2049) were obtained from the IPSL-CM6A-LR (45,46) global climate model (endorsed by CMIP6 (47)) under SSP1-2.6, SSP2-4.5, and SSP5-8.5. Five climate model realizations per SSP were used to account for internal model variability. Projections were bias-adjusted relative to ERA5-Land using an anomaly-based method (48–54) (appendix pp 9-10).

Adjacency matrices

To capture local spatial diffusion, we constructed adjacency matrices describing connections between neighbouring administrative units.

- **First-order adjacency** $A^{(1)}$ identified units sharing a common boundary.
- **Second-order adjacency** $A^{(2)}$ identified units separated by one intermediate neighbour.
- **Third-order adjacency** $A^{(3)}$ identified units separated by two intermediate neighbours.

Propagation model

The spatiotemporal propagation of *Aedes albopictus* was modeled using an invasion framework, inspired by (55,56). The model predicts yearly invasion probabilities for spatial units that are not yet invaded. The transition of a unit from uninvaded to invaded is irreversible.

For each uninvaded unit *j*, the force of invasion $\lambda_{i\to j,t}$ (FOI) in year t, defined as the instantaneous risk that it becomes invaded from an invaded unit *i* during year t combines two distinct mechanisms:

(i) a mobility-driven introduction pressure from unit *i*, $M_{i\to j,t}$ and

(ii) the local climatic suitability in unit *j* $S_{j,t}$

$$\lambda_{i\to j,t} = M_{i,j,t}.S_{j,t}$$

The total yearly FOI on unit *j* is expressed as the sum of the contributions $\lambda_{i\to j,t}$ of each of the spatial units *i* already invaded.

<u>Climatic suitability component</u>

Two alternative suitability formulations were tested. Both relied on climatic variables selected from known mosquito biological characteristics, and the second formulation additionally incorporated biologically informed functional responses derived from laboratory studies.

M0: polynomial dependence on the five climatic variables

$$S_{j,t} = (minT_{j,t})^{\epsilon}(medT_{j,t})^{\delta}(medRh_{j,t})^{\tau}(medSol_{j,t})^{\theta}(TotPrec_{j,t})^{\phi}$$

where all the parameters $\epsilon, \delta, \tau, \theta, \phi$ are unknown and estimated from the data.

M1-M5: Gaussian response to median temperature (reflecting experimentally established thermal optima (57)) combined with polynomial effects for the remaining variables:

$$S_{j,t} = (minT_{j,t})^{\epsilon} exp(\frac{-(medT_{j,t} - \mu_{temp})^2}{2\sigma_{temp}^2})(medRh_{j,t})^{\tau}(medSol_{j,t})^{\theta}(TotPrec_{j,t})^{\phi}$$

with $\epsilon, \tau, \theta, \phi, \mu_{temp}$ and σ_{temp} fitted to the data.

Mobility component

M0-M1: gravity model

The baseline mobility formulation (**M0-M1**) follows a gravity model and is expressed as:

$$M_{i,j,t} = \beta \frac{P_{i,t}^{\nu} P_{j,t}^{\mu}}{d_{i,j}^{\gamma}}$$

where $P_{i,t}$ and $P_{j,t}$ are the population sizes in units *i* and *j* at time step *t*, $d_{i,j}$ is the Euclidean distance (in km) between the centroids of *i* and *j*, and β, μ, ν and γ are estimated.

M2: gravity model and adjacency

To capture local diffusion, model **M2** adds adjacency-based transmission terms:

$$M_{i,j,t} = \beta \frac{P_{i,t}^{\nu} P_{j,t}^{\mu}}{d_{i,j}^{\gamma}} + \sum_{k=1}^{2} \alpha_k A_{i,j}^{(k)},$$

where adjacency coefficients α_k are also fitted. The combination of direct and second-order adjacency matrices performed best and was retained in adjacency-based models (**see Sensitivity analysis1**).

M3-M5: gravity model, adjacency and country borders

Models **M3–M5** incorporate border effects to account for reduced cross-border connectivity:

- **M3**: border effect applied to adjacency only:

  $$M_{i,j,t} = \beta \frac{P_{i,t}^{\nu} P_{j,t}^{\mu}}{d_{i,j}^{\gamma}} + (\sum_{k=1}^{2} \alpha_k A_{i,j}^{(k)}) e^{-\rho Borders_{i,j}},$$

  where ρ is an estimated friction parameter and the matrix entry ***Borders***$_{i,j}$ is equal to 1 if i and j are not in the same country and 0 otherwise.
- **M4:** shared border effect applied to gravity and adjacency terms:

  $$M_{i,j,t} = (\beta \frac{P_{i,t}^{\nu} P_{j,t}^{\mu}}{d_{i,j}^{\gamma}} + (\sum_{k=1}^{2} \alpha_k A_{i,j}^{(k)})) e^{-\rho Borders_{i,j}}$$

- **M5**: separate border effects for gravity and adjacency:

  $$M_{i,j,t} = \beta \frac{P_{i,t}^{\nu} P_{j,t}^{\mu}}{d_{i,j}^{\gamma}} e^{-\rho_1 Borders_{i,j}} + (\sum_{k=1}^{2} \alpha_k A_{i,j}^{(k)}) e^{-\rho_2 Borders_{i,j}}$$

All covariates from suitability and mobility components were normalized prior to inference.

Statistical inference and model comparison

Parameters were estimated within a Bayesian framework using a Metropolis–Hastings Markov chain Monte Carlo (MCMC) algorithm with lognormal proposal distributions. Broad uniform priors with biologically and epidemiologically plausible bounds were assigned to all parameters (appendix p 19). Model comparison was based on the Deviance Information Criterion (DIC) (58). We used the median posterior parameter estimates to simulate 100 datasets for each fitted model. In all simulations, the initial invasion sources were set to the first 10 invaded spatial units from the real dataset. Predictive performance was assessed using Brier scores (59) and Area Under the Curve (AUC) values under fixed-window cross-validation procedures (appendix pp 11-12)**.**

Projections of mosquito spread

Using posterior median estimates from our best model, we generated 100 projected trajectories for 2025-2049 under SSP1-2.6, SSP2-4.5, and SSP5-8.5. Scenario-specific climate and population projections were incorporated to estimate yearly local invasion probabilities. Therefore, separate sets of simulations were performed for each greenhouse-gas emission pathway: SSP1–2.6 (low emissions), SSP2–4.5 (medium emissions), and SSP5–8.5 (high emissions); and for each of five climate model realizations (r1i1p1f1, r2i1p1f1, r3i1p1f1, r4i1p1f1, and r6i1p1f1).

Role of the funder : The funder had no role in study design, data collection, data analysis, data interpretation, writing of the report, or decision to submit.

Results

Aedes albopictus was largely confined to Italy until 2000, after which its invasion expanded into southeastern France. By 2005, the species had become established in northern Spain and along the eastern Spanish coast, and had begun to invade the Netherlands. By 2015, *Aedes albopictus* was present in Germany, and by 2020 it had reached the United Kingdom. Scandinavian countries, which had remained largely unaffected by the species' expansion throughout most of the study period, reported their first detection in Sweden in 2023 (**Figure 1**).

Model performance, assessed using DIC, improved substantially with the progressive inclusion of additional mechanistic components (appendix p 21). Introducing a Gaussian relationship between suitability and median temperature significantly improved fit relative to the baseline (M0-M1: ΔDIC =10).

The inclusion of first and second orders adjacency-based transmission terms further enhanced performance (M1-M2: ΔDIC = 104), highlighting the importance of local neighbor influence. Adding a third order component did not improve fit (appendix p 22). Including a border effect within the adjacency term provided additional improvement (M2-M3: ΔDIC = 11).

Extending this border effect to the gravity-based human mobility component yielded further improvement (M3-M4: ΔDIC = 7), indicating that border effects influenced both short- and long-distance dispersal. Allowing separate border effects for adjacency and gravity terms reduced performance (M4- M5: ΔDIC = -6).

Model M4 was therefore selected as the best-performing model. Regarding spatial dynamics, all models except M0 reproduced the overall proportion of invaded areas (43%) across the 28 reconstructed years (1996-2024): M0 (54% 95%CI [46%, 61%]), M1 (47% 95%CI [39%, 53%]), M2 (38% 95%CI [28%, 46%]), M3 (41% 95%CI [31%, 50%]), M4 (41% 95%CI [30%, 52%]) and M5 (41% 95%CI [31%, 50%]) (appendix p 28).

The power coefficient associated with destination population sizes (0.133 95%CI [1.27e-02, 3.16e-01]) was more than eight times larger than the one associated with origin population sizes (1.61e-02 [5.31e-04, 8.38e-02]). Increasing the destination population size from 10,000 to 25,000 resulted in a 25% augmentation of the FOI, whereas an equivalent increase in the origin population size produced only marginal changes in the overall FOI (**Figure 2.A–B**).

The distance separating invaded and susceptible units strongly constrained the invasion risk. The power coefficient for normalized distances was estimated at 1.70 (95% CI: [1.52, 1.87]). As a result, increasing the inter-centroid distance between two spatial units from a reference distance of 100km to 500km resulted in an approximately eight-fold reduction of the force of invasion (**Figure 2.H**), underscoring the impact of the spatial structure on the mosquito's propagation. Direct adjacency further increased the invasion probability by roughly 7% per year, while secondary adjacency exerted a weaker but measurable effect, translating into an increase of approximately 1% in invasion probability per year. Crossing a country border reduced the FOI by nearly one-third, with an estimated border effect of ρ=0.985 (95%CI [0.50, 1.55]).

The power coefficient associated with minimum temperature was estimated at 5.38 (95% CI [0.33, 14.30]). Increasing the minimum temperatures from the median 0 °C (273K) to 7 °C (280K) resulted in an approximately 15% increase in the FOI (**Figure 2.C,** appendix pp 30-31). Median temperature during the dry season was a major driver of invasion dynamics, with FOI doubling as median temperatures rose from the median 15 °C (288K) to 22 °C (295K) (**Figure 2.G**). Relative humidity during the dry season exerted a strong influence, with an estimated power coefficient of 5.67 (95%CI [1.47, 10.10]). A 5% increase in relative humidity (from the median 90% to 95%) increases local suitability by 36% (**Figure 2.D**). The power coefficient of the total precipitation during the dry season was estimated at 0.107 (95%CI [4.90e-03, 3.48e-01]) (**Figure 2.E**). Finally, for surface solar radiation, the power parameter was estimated at 1.03 (95%CI [0.462, 1.71]), with the invasion pressure increasing by 40% as solar radiation increased from the median 18 to 25 MJ m^{-2} (**Figure 2.F**). A sensitivity analysis showed that the full model accounting for the effects of mobility and climatic suitability outperformed a mobility-only formulation in terms of model fit (DIC) and overall historical predictive performance (appendix p 24).

Our expansion model accurately reproduced the historical spread of *Aedes albopictus* in Europe. Performance was first evaluated qualitatively by visually comparing observed invasion maps with predicted probabilities over time, showing that the initial spread in Italy and subsequent expansion in France, Spain and the Balkans were well captured (**Figure 3**).

Quantitatively, the model demonstrated strong discriminatory ability, with fixed-window AUC values of 0.84 (training 1992–2012; testing 2013–2017) and 0.78 (training 1992–2018; testing 2019–2023) (appendix p 29, appendix p 36). Brier scores further confirmed the model's predictive accuracy, with mean values across European countries remaining below 0.05 throughout the study period. Only four years (2015, 2016, 2022, 2023) exceeded this threshold, yet all remained below 0.1, underscoring overall model reliability (appendix pp 32-35).

Mean invasion probabilities indicate a rapid expansion across Europe (**Figure 4.A**). Invasion probabilities are reported only for spatial units uninvaded at the end of 2024, allowing assessment of future risk of mosquito presence in currently unaffected areas. For all emission scenarios (SSP1–2.6, SSP2–4.5, SSP5–8.5), projected invasion trajectories were highly consistent across the five realizations of the climate model with identical forcing, indicating limited sensitivity to internal climate variability (appendix pp 37-38). Consequently, results for each of the three scenarios (SSP1-2.6, SSP2-4.5, SSP5-8.5) were obtained by averaging projections across realizations and reporting the associated 95% prediction intervals derived from the full ensemble of simulations (n = 500)..

Across all three climate scenarios, the model projects a marked increase in the proportion of the European population at risk of coming into contact with *Aedes albopictus*. The reported percentages correspond to the proportion of the population in the study area that is exposed, averaged across 500 simulated invasion trajectories. Specifically, the population at risk is predicted to rise from 49% in 2024 to 64% by 2030 under the scenario SSP2-4.5 (SSP1-2.6: 62%, SSP5-8.5: 63%). This increase accelerates over the following decade, reaching 84% by 2040 under scenario SSP2-4.5 (SSP1-2.6: 82%, SSP5-8.5: 81%). By the end of the projection period (2049), the proportion of the population at risk exceeds 90% under all scenarios, (SSP1-2.6: 90%, SSP2-4.5: 92%, SSP5-8.5: 91%) (**Figures 4.A and 4-B**).

A similar trend is observed for the spatial extent of invasion. Starting from 43% of European spatial units classified as invaded in 2024, the invaded area is projected to expand to 57% by 2030 under scenario SSP2-4.5 (SSP1-2.6: 55%, SSP5-8.5: 56%), increase to 75% by 2040 under the middle scenario (SSP1-2.6: 72%, SSP5-8.5: 72%), and exceed 80% by 2049 across all three scenarios, (SSP1-2.6: 80%, SSP2-4.5: 82%, SSP5-8.5: 81%) (**Figures 4.A and 4.C**).

At the country level, projections show strong consistency among scenarios in both the proportion of the population at risk of exposure to the mosquito and the percentage of invaded spatial units by 2049. Scenario SSP2-4.5 consistently yields slightly higher values, reflecting a modestly faster rate of spread, a pattern also evident in the overall dynamics of invasion (appendix pp 39-40, appendix pp 41-50). Based on the projected risk trajectories, countries can be classified into four distinct risk categories: countries already fully at risk, countries where risk is already present and continues to increase, countries currently free of invasion but projected to experience rising risk, and countries where risk remains persistently low (appendix p 51).

Discussion

In this study, we developed a unified mathematical framework to model the expansion of *Aedes albopictus* in Europe, by jointly inferring human-mediated introduction pressure and climatic suitability shaped by biological characteristics within a single likelihood. Unlike previous sequential or partially decoupled approaches, our joint inference propagates uncertainty consistently across processes, reduces overfitting to historical correlations, and preserves mechanistic interpretability when extrapolating beyond observed conditions. Among multiple tested formulations, a model combining gravity-based human mobility, short-range spatial diffusion, national border effects and five climatic variables informed by field and laboratory studies best explained the invasion dynamics over the past three decades.

Two complementary modelling approaches can be considered. First, a mathematical model that describes with great detail all the stages of mosquito life cycle may be calibrated to available experimental data on mosquito biology (76-78). It is then interesting to explore whether such a model can explain observed patterns of mosquito invasion. Such analysis is important to ascertain whether there is good adequacy between experimental and field data. However, even minor differences between experimental and field conditions might generate subtle differences in parameter regimes that could be sufficient to cause discrepancies between observed and expected invasion trajectories and suboptimal forecasts. In addition, these fully mechanistic models are computationally intensive, making their use very difficult for a study area as vast as the European continent. To tackle these challenges, we considered an alternative modelling strategy that identifies the parameter regime that best explains observed patterns of mosquito invasion and that can be applicable to a broad study area. The key philosophical difference is that we use experimental understanding of mosquito biology to identify which environmental variables are expected to affect the invasion process (and in some cases, the shape of the association), but parameters driving the impact are directly estimated by calibrating our model to the rich invasion dataset. By comparing our estimates of key parameters to those obtained from experimental data, we can also assess consistency between experimental and field data.

Our best model reproduced past expansion patterns with high accuracy (AUC 0.84 for 1992–2012 training / 2013–2017 testing; AUC 0.78 for 1992–2018 training / 2019–2023 testing), matching or exceeding previous studies (e.g.,(37): 0.73–0.86; (27): 0.82–0.91). Unlike (27), which relied on larger U.S. datasets before transfer to Europe, our model was trained and applied directly to European dataset while simultaneously integrating introduction and establishment processes rather than modelling them separately. Additional comparison to other approaches based on correlative habitat suitability or species distribution models (73-75) is limited, as their evaluation metrics (AUC) primarily measure discriminatory power between presence and background rather than predictive performance of temporal invasion dynamics, and are therefore not directly comparable to our framework. Nevertheless, these studies broadly agree qualitatively on the predicted climatic suitability of southern and central Europe and the potential for northward expansion.

Human-mediated dispersal was key for the spatial expansion of *Aedes albopictus* in Europe. Human mobility, modeled through a gravity-based formulation, emerged as a major driver of spread, in agreement with previous studies (27,36,38,60). At shorter distances, spatial adjacency played a critical role. These values confirm that short-range diffusion is a key mechanism of *Aedes albopictus* spread, in line with (27,37,61). A strong border effect

between countries was also identified, indicating that national borders significantly constrain dispersal through their impact on human movement. This contrasts with the findings of (27), who did not detect such an effect, likely due to their US-calibrated framework.

Climatic suitability constitutes a major determinant of expansion. Our best model identified five variables, minimum and median temperature, relative humidity, total precipitation, and median solar radiation, which together maximized predictive performance. While prior studies identified overlapping predictors (median and minimum temperatures, humidity in (37), minimum and maximum temperatures, precipitation, humidity in (27)), our sensitivity analyses showed that including precipitation and minimum temperature improved performance (appendix p 23), consistent with (61–63). Together, these covariates capture key biological constraints on survival, development, and persistence of the mosquitoes. Overall, the estimated climatic responses were consistent with laboratory-based evidence, including an optimal median temperature for mosquito development close to 32°C (68), as well as well-established physiological constraints governing its life cycle (66-72). In particular, the model reproduced key experimentally documented effects: the influence of minimum temperature on processes such as egg diapause and overwintering survival, the role of humidity and precipitation in shaping larval habitat availability, and the impact of solar radiation on egg hatching (Figure 2). Taken together, these agreements support the biological plausibility of the inferred relationships and highlight consistency between field-based calibration and experimental findings. Although we did not explicitly include a seasonality metric, minimum temperature partly captures winter constraints on survival and overwintering, while median temperature reflects overall thermal suitability, thereby indirectly accounting for key seasonal limitations on mosquito persistence.

Projections under multiple climate scenarios indicate rapid and widespread expansion: the population at risk of being exposed to *Aedes albopictus* increases from 49% currently to over 90% within 25 years, and invaded spatial units increase from 43% to more than 80% by 2049. These projections are broader than those made by Kraemer et al. (27). Several reasons could explain the faster and more extensive invasion projected here. Contrary to Kraemer et al., in our model, expansion results from the interaction of the two components climatic suitability and human mediated dispersal, instead of each of them acting independently, which is more aligned with real invasion dynamics. Also, Kraemer et al. used a model trained on US data to project future European expansion. However, dispersal ability as well as suitable climatic conditions for expansion may differ between the two mosquito populations. The similarity of invasion trajectories across different emission scenarios reflects the relative similarity of the projected climatic conditions over the next 25 years, and not a limited role of climate, as confirmed by the superior performance of the full model over the mobility-only formulation (appendix p 24).
Projected dynamics are spatially heterogeneous. Countries fall into four categories: already fully at risk of mosquito presence, increasing risk, emerging risk, and persistently low risk. Uncertainty is substantially higher at the country level, especially in countries not yet invaded today, as projections depend on stochastic introduction events whose occurrence and timing determine whether and how rapidly spread unfolds. This classification captures temporal and spatial heterogeneity and provides actionable guidance for surveillance, vector control, and preparedness, particularly given epidemiological evidence that arboviral outbreaks typically follow mosquito invasion within a decade.

Our work has several limitations. First, some environmental factors known to influence *Aedes albopictus* establishment were not included. Some studies explored the role of wind in mosquito dispersal. Wind-driven movement is more appropriate for modelling local dispersal processes at fine spatial scales and was therefore not included in our large-scale expansion model. Similarly, land use, vegetation cover, and elevation have been shown to affect the mosquito presence and abundance. However the NUTS level is too coarse to represent local habitat heterogeneity or barriers to movement. The spatial resolution of the data also limits the identification of local heterogeneities in mosquito invasion, which tend to be concentrated around urban centers within spatial units (79), thereby potentially overestimating the population at risk within each spatial unit. Second, our framework models the timing of invasion events and cannot capture post-establishment dynamics. In this setting, invaded spatial units become the drivers of further spread to neighbouring areas, and it is this temporal sequence of invasion and the resulting propagation structure, rather than local declines or reversals in suitability under changing climate conditions, that is central to the dynamics and captured by our model. We also do not distinguish between transient introductions and long-term establishment. Once a spatial unit is recorded as invaded, it is assumed to remain so until the end of the study period. Consequently, some transient occurrences may be classified as invasions despite not leading to sustained establishment. However, such cases appear rare, as explicitly recorded transitions from invaded to uninvaded status represented less than 1% of surveillance records that were removed from the data. This suggests a negligible impact on the large-scale spatiotemporal patterns described here. Additionally, the model does not account for potential additional introductions from outside of Europe or the circulation of genetically distinct *Aedes albopictus* subpopulations, which may influence regional invasion dynamics. Fourth, in our model, pseudo-absences were treated as true absences, an assumption that could be leveraged by drawing latent dates of invasion in some areas, within a Bayesian reversible-jump MCMC framework (64). Moreover, our analysis does not explicitly model sampling effort or detection bias. As shown by (27,38), variation in surveillance intensity can influence presence–absence records. Incorporating an observation process or a sampling-effort model represents a promising extension of our framework. Sixth, although the first European record of *Aedes albopictus* is widely recognized to be from Albania in 1979, this introduction was not represented in the occurrence datasets used for model initialization, which instead identified Italy as the earliest source region. Given Albania's marked isolation under the dictatorial communist regime at the time, this introduction was unlikely to have played a major role in the species' subsequent spread across Europe and was therefore not added manually. However, its omission may have contributed to the lower accuracy of the model in reproducing invasion dynamics in parts of the Balkans. Finally, in our study, we relied on a single climate model (IPSL-CM6A-LR) to ensure structural consistency across projections, while using multiple realizations to explicitly capture internal variability within a physically coherent climate modelling framework. Future work could apply our approach to project *Aedes albopictus* expansion using alternative climate models, in order to assess uncertainties arising from inter-model differences (80).

Despite these limitations, the strengths of our study lie in the integration of biologically grounded climatic covariates, the explicit modelling of both short- and long-range human-mediated dispersal, and the identification of national borders as a significant constraint on spread, within a computationally efficient model. It enables continent-scale inference within hours and instantaneous projections once fitted. The model’s ability to

predict future expansion and identify the population at risk of being in contact with *Aedes albopictus* in the next 25 years makes it directly relevant for public health preparedness. This model could be used to inform targeted surveillance, early intervention, vector control prioritization and anticipatory planning for arbovirus prevention in Europe over the coming decades.

Contributors

CP data curation, formal analysis, investigation, methodology, validation, visualisation, writing – original draft, and writing– review & editing
AV data curation, validation, visualisation, writing – original draft, and writing– review & editing
JP data curation
CT writing– review & editing
MK writing– review & editing
PB conceptualisation, investigation, methodology, supervision, validation, visualisation, writing – original draft, and writing– review & editing.
SC conceptualisation, funding acquisition, investigation, methodology, supervision, validation, visualisation, writing – original draft, and writing– review & editing.
All authors had access to the data and reviewed and approved the final manuscript.

Declaration of interests

The authors declare no competing interests.

Data sharing

All data used in this study will be made available on a public repository upon acceptance of the article.

Acknowledgments: SC acknowledges support from the European Commission under the EU4Health programme 2021-2027, Grant Agreement - Project: 101102733 — DURABLE, the Laboratoire d'Excellence Integrative Biology of Emerging Infectious Diseases program (grant ANR-10-LABX-62-IBEID), the INCEPTION project (PIA/ANR16-CONV-0005) and the European Commission Horizon Europe program (LEAPS project #101094685, call *HORIZON-HLTH-2022-DISEASE-07).* AV acknowledges partial support from the chair programme *Mathematical modelling and biodiversity* (Ecole Polytechnique, Museum National d'Histoire Naturelle, Veolia Environnement, Fondation X). The authors would like to thank Jean-Noël Thépaut and Julie Deshayes for insightful discussions on climate projections and for their help to access the IPSL-CM6A-LR realizations.

1. Vector-borne diseases [Internet]. [cited 2026 Jan 6]. Available from: https://www.who.int/news-room/fact-sheets/detail/vector-borne-diseases

2. Bonizzoni M, Gasperi G, Chen X, James AA. The invasive mosquito species Aedes albopictus: current knowledge and future perspectives. Trends Parasitol. 2013 Sep;29(9):460–8. doi:10.1016/j.pt.2013.07.003 PubMed PMID: 23916878; PubMed Central PMCID: PMC3777778.

3. Gratz NG. Critical review of the vector status of Aedes albopictus. Med Vet Entomol. 2004 Sep;18(3):215–27. doi:10.1111/j.0269-283X.2004.00513.x PubMed PMID: 15347388.

4. Nsoesie EO, Kraemer MU, Golding N, Pigott DM, Brady OJ, Moyes CL, et al. Global distribution and environmental suitability for chikungunya virus, 1952 to 2015. Euro Surveill Bull Eur Sur Mal Transm Eur Commun Dis Bull. 2016 May 19;21(20). doi:10.2807/1560-7917.ES.2016.21.20.30234 PubMed PMID: 27239817; PubMed Central PMCID: PMC4902126.

5. Messina JP, Kraemer MU, Brady OJ, Pigott DM, Shearer FM, Weiss DJ, et al. Mapping global environmental suitability for Zika virus. Jit M, editor. eLife. 2016 Apr 19;5:e15272. doi:10.7554/eLife.15272

6. Bhatt S, Gething PW, Brady OJ, Messina JP, Farlow AW, Moyes CL, et al. The global distribution and burden of dengue. Nature. 2013 Apr;496(7446):504–7. doi:10.1038/nature12060

7. Lessler J, Chaisson LH, Kucirka LM, Bi Q, Grantz K, Salje H, et al. Assessing the global threat from Zika virus. Science. 2016 Aug 12;353(6300):aaf8160. doi:10.1126/science.aaf8160 PubMed PMID: 27417495; PubMed Central PMCID: PMC5467639.

8. Kraemer MUG, Sinka ME, Duda KA, Mylne A, Shearer FM, Brady OJ, et al. The global compendium of Aedes aegypti and Ae. albopictus occurrence. Sci Data. 2015;2:150035. doi:10.1038/sdata.2015.35 PubMed PMID: 26175912; PubMed Central PMCID: PMC4493829.

9. Enserink, M. (2008). A mosquito goes global. Science 320(5878), 864–866. - Recherche Google [Internet]. [cited 2026 Jan 6]. Available from: https://www.google.com/search?client=safari&rls=en&q=Enserink%2C+M.+(2008).+A+mosquito+goes+global.+Science+320(5878)%2C+864%E2%80%93866.&ie=UTF-8&oe=UTF-8

10. Darbro J, Halasa Y, Montgomery B, Muller M, Shepard D, Devine G, et al. An Economic Analysis of the Threats Posed by the Establishment of *Aedes albopictus* in Brisbane, Queensland. Ecol Econ. 2017 Dec 1;142:203–13. doi:10.1016/j.ecolecon.2017.06.015

11. Farooq Z, Segelmark L, Rocklöv J, Lillepold K, Sewe MO, Briet OJT, et al. Impact of climate and Aedes albopictus establishment on dengue and chikungunya outbreaks in Europe: a time-to-event analysis. Lancet Planet Health. 2025 May;9(5):e374–83. doi:10.1016/S2542-5196(25)00059-2 PubMed PMID: 40381632.

12. Paupy C, Delatte H, Bagny L, Corbel V, Fontenille D. Aedes albopictus, an arbovirus vector: from the darkness to the light. Microbes Infect. 2009 Dec;11(14–15):1177–85. doi:10.1016/j.micinf.2009.05.005 PubMed PMID: 19450706.

13. Madon MB, Mulla MS, Shaw MW, Kluh S, Hazelrigg JE. Introduction of Aedes albopictus (Skuse) in southern California and potential for its establishment. J Vector Ecol J Soc Vector Ecol. 2002 Jun;27(1):149–54. PubMed PMID: 12125866.

14. Scholte EJ, Dijkstra E, Blok H, De Vries A, Takken W, Hofhuis A, et al. Accidental importation of the mosquito Aedes albopictus into the Netherlands: a survey of mosquito distribution and the presence of dengue virus. Med Vet Entomol. 2008 Dec;22(4):352–8. doi:10.1111/j.1365-2915.2008.00763.x PubMed PMID: 19120963.

15. Demeulemeester J, Deblauwe I, Witte J, Jansen F, Hendy A, Madder M. First interception of Aedes (Stegomyia) albopictus in Lucky bamboo shipments in Belgium. J Eur Mosq Control Assoc. 2014 May 9;JEMCA:14–6.

16. Powell JR, Tabachnick WJ. History of domestication and spread of Aedes aegypti--a review. Mem Inst Oswaldo Cruz. 2013;108 Suppl 1(Suppl 1):11–7. doi:10.1590/0074-0276130395 PubMed PMID: 24473798; PubMed Central PMCID: PMC4109175.

17. Scott TW, Amerasinghe PH, Morrison AC, Lorenz LH, Clark GG, Strickman D, et al. Longitudinal studies of Aedes aegypti (Diptera: Culicidae) in Thailand and Puerto Rico: blood feeding frequency. J Med Entomol. 2000 Jan;37(1):89–101. doi:10.1603/0022-2585-37.1.89 PubMed PMID: 15218911.

18. Benelli G, Wilke ABB, Beier JC. Aedes albopictus (Asian Tiger Mosquito). Trends Parasitol. 2020 Nov;36(11):942–3. doi:10.1016/j.pt.2020.01.001 PubMed PMID: 32037135.

19. Armbruster PA. Photoperiodic Diapause and the Establishment of Aedes albopictus (Diptera: Culicidae) in North America. J Med Entomol. 2016 Sep;53(5):1013–23. doi:10.1093/jme/tjw037 PubMed PMID: 27354438; PubMed Central PMCID: PMC5013814.

20. Hawley WA. The biology of Aedes albopictus. J Am Mosq Control Assoc Suppl. 1988 Dec;1:1–39. PubMed PMID: 3068349.

21. Maynard AJ, Ambrose L, Cooper RD, Chow WK, Davis JB, Muzari MO, et al. Tiger on the prowl: Invasion history and spatio-temporal genetic structure of the Asian tiger mosquito Aedes albopictus (Skuse 1894) in the Indo-Pacific. PLoS Negl Trop Dis. 2017 Apr 14;11(4):e0005546. doi:10.1371/journal.pntd.0005546

22. Adhami J, Reiter P. Introduction and establishment of Aedes (Stegomyia) albopictus skuse (Diptera: Culicidae) in Albania. J Am Mosq Control Assoc. 1998 Sep;14(3):340–3. PubMed PMID: 9813831.

23. Caminade C, Medlock JM, Ducheyne E, McIntyre KM, Leach S, Baylis M, et al. Suitability of European climate for the Asian tiger mosquito Aedes albopictus: recent trends and future scenarios. J R Soc Interface. 2012 Oct 7;9(75):2708–17. doi:10.1098/rsif.2012.0138 PubMed PMID: 22535696; PubMed Central PMCID: PMC3427500.

24. Aedes albopictus - current known distribution: October 2023 [Internet]. 2023 [cited 2026 Jan 6]. Available from: https://www.ecdc.europa.eu/en/publications-data/aedes-albopictus-current-known-distribution-october-2023

25. Metelmann S, Caminade C, Jones AE, Medlock JM, Baylis M, Morse AP. The UK's suitability for Aedes albopictus in current and future climates. J R Soc Interface. 2019 Mar 13;16(152):20180761. doi:10.1098/rsif.2018.0761

26. Torina A, La Russa F, Blanda V, Peralbo-Moreno A, Casades-Martí L, Di Pasquale L, et al. Modelling time-series *Aedes albopictus* abundance as a forecasting tool in urban environments. Ecol Indic. 2023 Jun 1;150:110232. doi:10.1016/j.ecolind.2023.110232

27. Kraemer MUG, Reiner RC, Brady OJ, Messina JP, Gilbert M, Pigott DM, et al. Past and future spread of the arbovirus vectors Aedes aegypti and Aedes albopictus. Nat Microbiol. 2019 May;4(5):854–63. doi:10.1038/s41564-019-0376-y PubMed PMID: 30833735; PubMed Central PMCID: PMC6522366.

28. Medlock JM, Avenell D, Barrass I, Leach S. Analysis of the potential for survival and seasonal activity of Aedes albopictus (Diptera: Culicidae) in the United Kingdom. J Vector Ecol J Soc Vector Ecol. 2006 Dec;31(2):292–304. doi:10.3376/1081-1710(2006)31[292:aotpfs]2.0.co;2 PubMed PMID: 17249347.

29. Tran A, L'Ambert G, Lacour G, Benoît R, Demarchi M, Cros M, et al. A Rainfall- and Temperature-Driven Abundance Model for Aedes albopictus Populations. Int J Environ Res Public Health. 2013 Apr 26;10(5):1698–719. doi:10.3390/ijerph10051698

30. Strugarek M, Vauchelet N, Zubelli JP. Quantifying the survival uncertainty of Wolbachia-infected mosquitoes in a spatial model. Math Biosci Eng MBE. 2018 Aug 1;15(4):961–91. doi:10.3934/mbe.2018043 PubMed PMID: 30380317.

31. Haramboure M, Labbé P, Baldet T, Damiens D, Gouagna LC, Bouyer J, et al. Modelling the control of Aedes albopictus mosquitoes based on sterile males release techniques in a tropical environment. Ecol Model. 2020 May;424:109002. doi:10.1016/j.ecolmodel.2020.109002

32. Tran A, Mangeas M, Demarchi M, Roux E, Degenne P, Haramboure M, et al. Complementarity of empirical and process-based approaches to modelling mosquito population dynamics with Aedes albopictus as an example—Application to the development of an operational mapping tool of vector populations. PLOS ONE. 2020 Jan 17;15(1):e0227407. doi:10.1371/journal.pone.0227407

33. Dufourd C, Dumont Y. Modeling and Simulations of Mosquito Dispersal. The Case of Aedes albopictus. BIOMATH. 2012 Dec 31;1. doi:10.11145/j.biomath.2012.09.262

34. Roques L, Bonnefon O. Modelling Population Dynamics in Realistic Landscapes with Linear Elements: A Mechanistic-Statistical Reaction-Diffusion Approach. PloS One. 2016;11(3):e0151217. doi:10.1371/journal.pone.0151217 PubMed PMID: 26986201; PubMed Central PMCID: PMC4795701.

35. He W, Richter O. Modelling Large Scale Invasion of Aedes aegypti and Aedes albopictus Mosquitoes. Adv Pure Math. 2018 Mar 14;8(3):245–65. doi:10.4236/apm.2018.83013

36. Richter O, Nguyen A, Nguyen T. Application of reaction-diffusion equations for modeling human and breeding site attraction movement behavior of Aedes aegypti mosquito. Math Biosci Eng MBE. 2022 Sep 5;19(12):12915–35. doi:10.3934/mbe.2022603 PubMed PMID: 36654028.

37. Barman S, Semenza JC, Singh P, Sjödin H, Rocklöv J, Wallin J. A climate and population dependent diffusion model forecasts the spread of Aedes Albopictus mosquitoes in Europe. Commun Earth Environ. 2025 Apr 9;6(1):276. doi:10.1038/s43247-025-02199-z

38. Roques L, Boivin T, Papaïx J, Soubeyrand S, Bonnefon O. Dynamics of Aedes albopictus invasion insights from a spatio-temporal model. Biol Invasions. 2023 Apr. doi:10.1007/s10530-023-03062-y

39. VectorNet [Internet]. [cited 2026 Jan 6]. Available from: https://www.vectornetdata.org/

40. UNCCD [Internet]. [cited 2026 Jan 6]. Socio Economic Data Applications Center (SEDAC). Available from: https://www.unccd.int/resources/knowledge-sharing-system/socio-economic-data-applications-center-sedac

41. WorldPop [Internet]. [cited 2026 Jan 6]. Open Spatial Demographic Data and Research. Available from: https://www.worldpop.org/

42. Accueil - Eurostat [Internet]. [cited 2026 Jan 6]. Available from: https://ec.europa.eu/eurostat/fr/

43. Wang X, Meng X, Long Y. Projecting 1 km-grid population distributions from 2020 to 2100 globally under shared socioeconomic pathways. Sci Data. 2022 Sep 12;9(1):563. doi:10.1038/s41597-022-01675-x

44. Climate Data Store [Internet]. [cited 2026 Jan 6]. Available from: https://cds.climate.copernicus.eu/

45. IPSL-CM6A-LR – My CMS [Internet]. [cited 2026 Jan 6]. Available from: https://cmc.ipsl.fr/ipsl-climate-models/ipsl-cm6/

46. Presentation and Evaluation of the IPSL-CM6A-LR Climate Model - Boucher - 2020 - Journal of Advances in Modeling Earth Systems - Wiley Online Library [Internet]. [cited 2026 Jan 6]. Available from: https://agupubs.onlinelibrary.wiley.com/doi/10.1029/2019MS002010

47. CMIP Phase 6 (CMIP6) - Coupled Model Intercomparison Project [Internet]. 2022 Dec 2 [cited 2026 Jan 6]. Available from: https://wcrp-cmip.org/cmip-phases/cmip6/

48. Andréasson J, Bergström S, Carlsson B, Graham LP, Lindström G. Hydrological Change – Climate Change Impact Simulations for Sweden. AMBIO J Hum Environ. 2004 Jun;33(4):228–34. doi:10.1579/0044-7447-33.4.228

49. Bosshard T, Carambia M, Goergen K, Kotlarski S, Krahe P, Zappa M, et al. Quantifying uncertainty sources in an ensemble of hydrological climate-impact projections. Water Resour Res. 2013;49(3):1523–36. doi:10.1029/2011WR011533

50. Gellens D, Roulin E. Streamflow response of Belgian catchments to IPCC climate change scenarios. J Hydrol. 1998 Sep 1;210(1):242–58. doi:10.1016/S0022-1694(98)00192-9

51. Lettenmaier DP, Wood AW, Palmer RN, Wood EF, Stakhiv EZ. Water Resources Implications of Global Warming: A U.S. Regional Perspective. Clim Change. 1999 Nov 1;43(3):537–79. doi:10.1023/A:1005448007910

52. Middelkoop H, Daamen K, Gellens D, Grabs W, Kwadijk JCJ, Lang H, et al. Impact of Climate Change on Hydrological Regimes and Water Resources Management in the Rhine Basin. Clim Change. 2001 Apr 1;49(1):105–28. doi:10.1023/A:1010784727448

53. Moore K, Pierson D, Pettersson K, Schneiderman E, Samuelsson P. Effects of warmer world scenarios on hydrologic inputs to Lake Mälaren, Sweden and implications for nutrient loads. In: Nõges T, Eckmann R, Kangur K, Nõges P, Reinart A, Roll G, et al., editors. European Large Lakes Ecosystem changes and their ecological and socioeconomic impacts [Internet]. Dordrecht: Springer Netherlands; 2008 [cited 2026 Jan 6]. p. 191–9. Available from: https://doi.org/10.1007/978-1-4020-8379-2_23 doi:10.1007/978-1-4020-8379-2_23

54. Shabalova M, van Deursen W, Buishand T. Assessing future discharge of the river Rhine using regional climate model integrations and a hydrological model. Clim Res. 2003;23:233–46. doi:10.3354/cr023233

55. Eggo RM, Cauchemez S, Ferguson NM. Spatial dynamics of the 1918 influenza pandemic in England, Wales and the United States. J R Soc Interface. 2011 Feb;8(55):233–43.

56. Perlant C, Weill FX, Paireau J, Scipioni M, Bosetti P, Cauchemez S. Modeling the spatio-temporal spread of cholera in France in 1892. Epidemics. 2025 Dec 1;53:100872. doi:10.1016/j.epidem.2025.100872

57. Doeurk B, Leng S, Long Z, Maquart PO, Boyer S. Impact of temperature on survival, development and longevity of Aedes aegypti and Aedes albopictus (Diptera: Culicidae) in Phnom Penh, Cambodia. Parasit Vectors. 2025 Aug 27;18:362. doi:10.1186/s13071-025-06892-y PubMed PMID: 40867007; PubMed Central PMCID: PMC12382174.

58. Meyer R. Deviance Information Criterion (DIC). In: Wiley StatsRef: Statistics Reference Online [Internet]. John Wiley & Sons, Ltd; 2016 [cited 2026 Jan 6]. p. 1–6. Available from: https://onlinelibrary.wiley.com/doi/abs/10.1002/9781118445112.stat07878 doi:10.1002/9781118445112.stat07878

59. Rufibach K. Use of Brier score to assess binary predictions. J Clin Epidemiol. 2010 Aug;63(8):938–9. doi:10.1016/j.jclinepi.2009.11.009

60. Da Re D, Van Bortel W, Reuss F, Müller R, Boyer S, Montarsi F, et al. dynamAedes: a unified modelling framework for invasive Aedes mosquitoes. Parasit Vectors. 2022 Nov 8;15(1):414. doi:10.1186/s13071-022-05414-4

61. Stone CM, Zuo Z, Li B, Ruiz M, Swanson J, Hunt J, et al. Spatial, Temporal, and Genetic Invasion Dynamics of Aedes albopictus (Diptera: Culicidae) in Illinois. J Med Entomol. 2020 Sep 7;57(5):1488–500. doi:10.1093/jme/tjaa047 PubMed PMID: 32195543.

62. Roche B, Léger L, L'Ambert G, Lacour G, Foussadier R, Besnard G, et al. The Spread of Aedes albopictus in Metropolitan France: Contribution of Environmental Drivers and Human Activities and Predictions for a Near Future. PloS One. 2015;10(5):e0125600. doi:10.1371/journal.pone.0125600 PubMed PMID: 25962160; PubMed Central PMCID: PMC4427491.

63. Carbajo AE, Cardo MV, Vezzani D. Past, present and future of *Aedes aegypti* in its South American southern distribution fringe: What do temperature and population tell us? Acta Trop. 2019 Feb 1;190:149–56. doi:10.1016/j.actatropica.2018.11.017

64. GREEN PJ. Reversible jump Markov chain Monte Carlo computation and Bayesian model determination. Biometrika. 1995 Dec 1;82(4):711–32. doi:10.1093/biomet/82.4.711

65. Director E, Opérationnelle G. Autorité européenne de sécurité des aliments. [cited 2026 May 6]. Autorité européenne de sécurité des aliments. Available from: https://www.efsa.europa.eu/fr

66. Thomas SM, Obermayr U, Fischer D, Kreyling J, Beierkuhnlein C. Low-temperature threshold for egg survival of a post-diapause and non-diapause European aedine strain, Aedes albopictus (Diptera: Culicidae). Parasites & vectors [Internet]. 2012 May 23 [cited 2026 Jun 28];5. Available from: https://pubmed.ncbi.nlm.nih.gov/22621367/

67. Brady OJ, Johansson MA, Guerra CA, Bhatt S, Golding N, Pigott DM, et al. Modelling adult Aedes aegypti and Aedes albopictus survival at different temperatures in

laboratory and field settings. Parasites & vectors [Internet]. 2013 Dec 12 [cited 2026 Jun 28];6. Available from: https://pubmed.ncbi.nlm.nih.gov/24330720/

68. Brady OJ, Golding N, Pigott DM, Kraemer MUG, Messina JP, Reiner RC Jr, et al. Global temperature constraints on Aedes aegypti and Ae. albopictus persistence and competence for dengue virus transmission. Parasit Vectors. 2014 Jul 22;7:338.

69. Delatte H, Gimonneau G, Triboire A, Fontenille D. Influence of temperature on immature development, survival, longevity, fecundity, and gonotrophic cycles of Aedes albopictus, vector of chikungunya and dengue in the Indian Ocean. Journal of medical entomology [Internet]. 2009 Jan [cited 2026 Jun 28];46(1). Available from: https://pubmed.ncbi.nlm.nih.gov/19198515/

70. Juliano SA, O'Meara GF, Morrill JR, Cutwa MM. Desiccation and thermal tolerance of eggs and the coexistence of competing mosquitoes. Oecologia. 2002 Feb 1;130(3):458–69.

71. Armbruster PA. Photoperiodic Diapause and the Establishment of Aedes albopictus (Diptera: Culicidae) in North America. Journal of medical entomology [Internet]. 2016 Sep [cited 2026 Jun 28];53(5). Available from: https://pubmed.ncbi.nlm.nih.gov/27354438/

72. Yee DA, Juliano SA, Vamosi SM. Seasonal photoperiods alter developmental time and mass of an invasive mosquito, Aedes albopictus (Diptera: Culicidae), across its north-south range in the United States. J Med Entomol. 2012 Jul;49(4):825–32.

73. Cunze S, Kochmann J, Koch LK, Klimpel S. Aedes albopictus and Its Environmental Limits in Europe. PLoS One. 2016 Sep 7;11(9):e0162116.

74. Proestos Y, Christophides GK, Ergüler K, Tanarhte M, Waldock J, Lelieveld J. Present and future projections of habitat suitability of the Asian tiger mosquito, a vector of viral pathogens, from global climate simulation. Philos Trans R Soc Lond B Biol Sci. 2015 Apr 5;370(1665):20130554.

75. Georgiades P, Proestos Y, Lelieveld J, Erguler K. Machine learning modeling of Aedes albopictus habitat suitability in the 21st century. Insects. 2023 May 9;14(5):447.

76. Pasquali S, Mariani L, Calvitti M, Moretti R, Ponti L, Chiari M, et al. Development and calibration of a model for the potential establishment and impact of Aedes albopictus in Europe. Acta Trop. 2020 Feb 1;202(105228):105228.

77. Lutambi AM, Penny MA, Smith T, Chitnis N. Mathematical modelling of mosquito dispersal in a heterogeneous environment. Math Biosci. 2013 Feb 1;241(2):198–216.

78. Roques L, Boivin T, Papaïx J, Soubeyrand S, Bonnefon O. Dynamics of Aedes albopictus invasion insights from a spatio-temporal model. Biol Invasions. 2024 Aug;25(8):2679–95.

79. Chikungunya, dengue et Zika - Données de la surveillance renforcée en France hexagonale 2025 [Internet]. [cited 2026 Jun 28]. Available from: https://www.santepubliquefrance.fr/maladies-a-transmission-vectorielle/chikungunya/chikungunya-dengue-zika-et-west-nile-donnees-de-la-surveillance-renforcee-en-france-hexagonale-2025

80. Hawkins E, Sutton R. The potential to narrow uncertainty in regional climate predictions. Bull Am Meteorol Soc. 2009 Aug 1;90(8):1095–108.

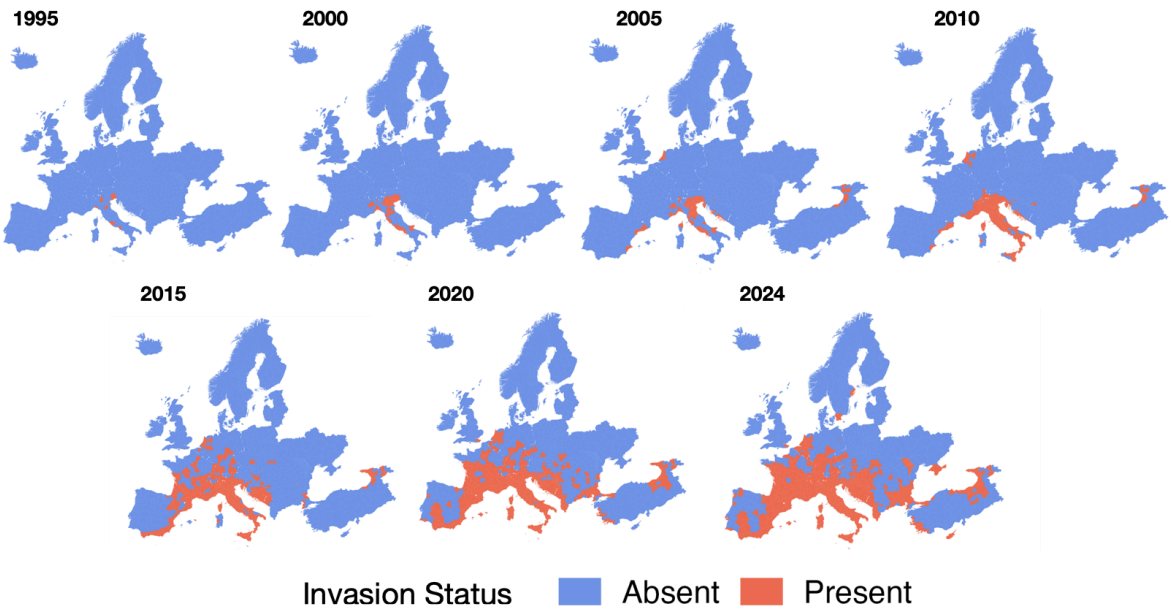

Figure 1. Maps of European spatiotemporal expansion of *Aedes albopictus*. Temporal evolution of *Aedes albopictus* invasion across Europe from 1995 to 2025, illustrated at 5-year intervals. Areas shown in blue are free of the mosquito, while red areas correspond to regions invaded by the species.

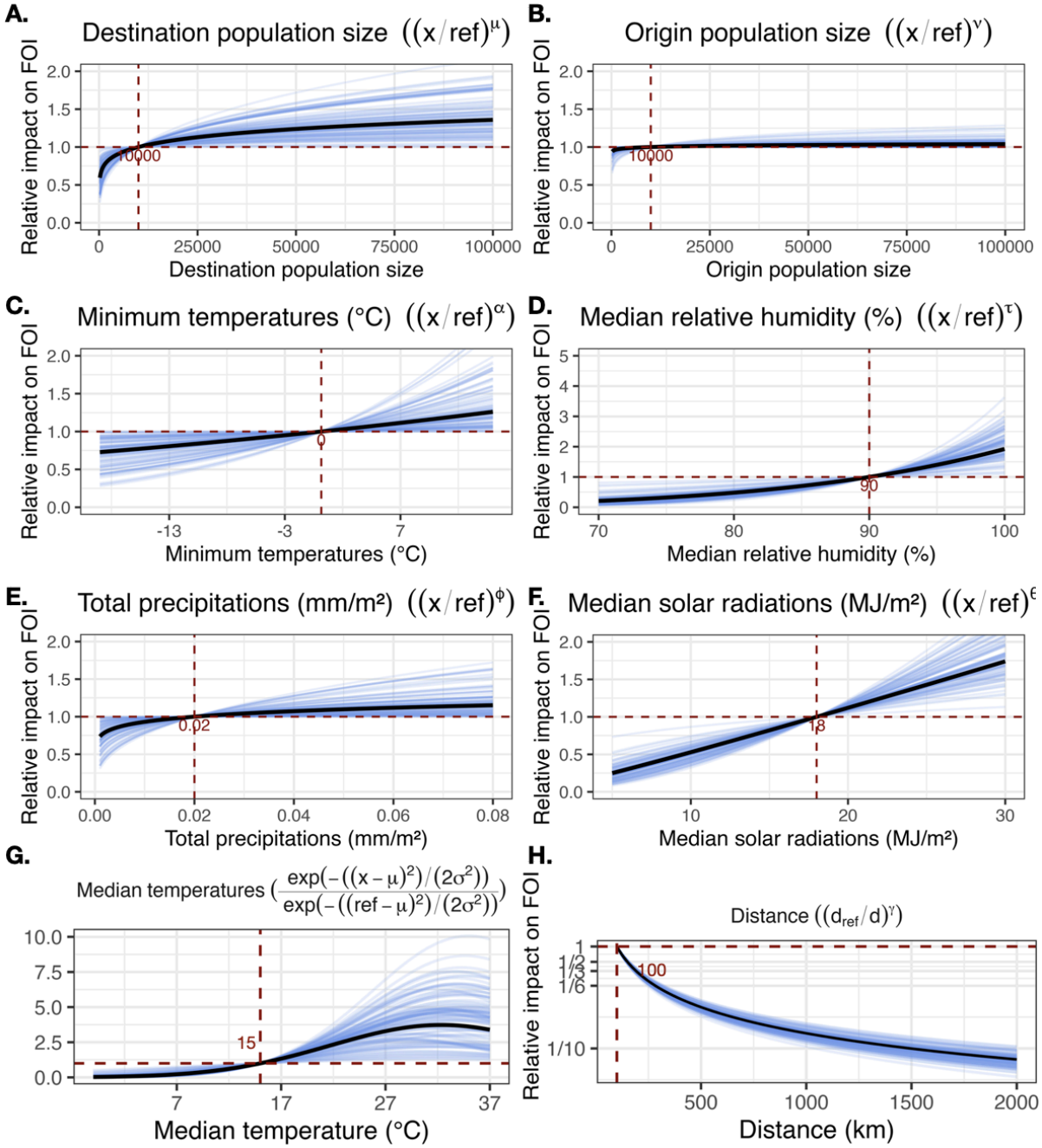

Figure 2. Effects of population sizes, distance and climatic variables on the FOI. Relative contributions of demographic, climatic, and distance variables to the force of invasion. The black curve shows the relative impact of each variable on the FOI, with a parameter equal to the median of its estimated posterior distribution. Blue curves correspond to the same impact computed from random draws of the parameter value from the estimated posterior distribution. All curves are normalized to a reference value, indicated by the vertical red dashed line.

A. Destination population size, relative to a reference of 10,000 inhabitants. **B.** Origin population size, relative to a reference of 10,000 inhabitants. **C.** Minimum temperature, relative to a reference of 0 °C. **D.** Median relative humidity, relative to a reference of 90%. **E.** Total precipitation, relative to a reference of 0.02 $mm.m^{-2}$. **F.** Median surface solar radiation, relative to a reference of 18 $MJ.m^{-2}$. **G.** Median temperature, relative to a reference of 15 °C. **H.** Distance, relative to a reference of 100 km.

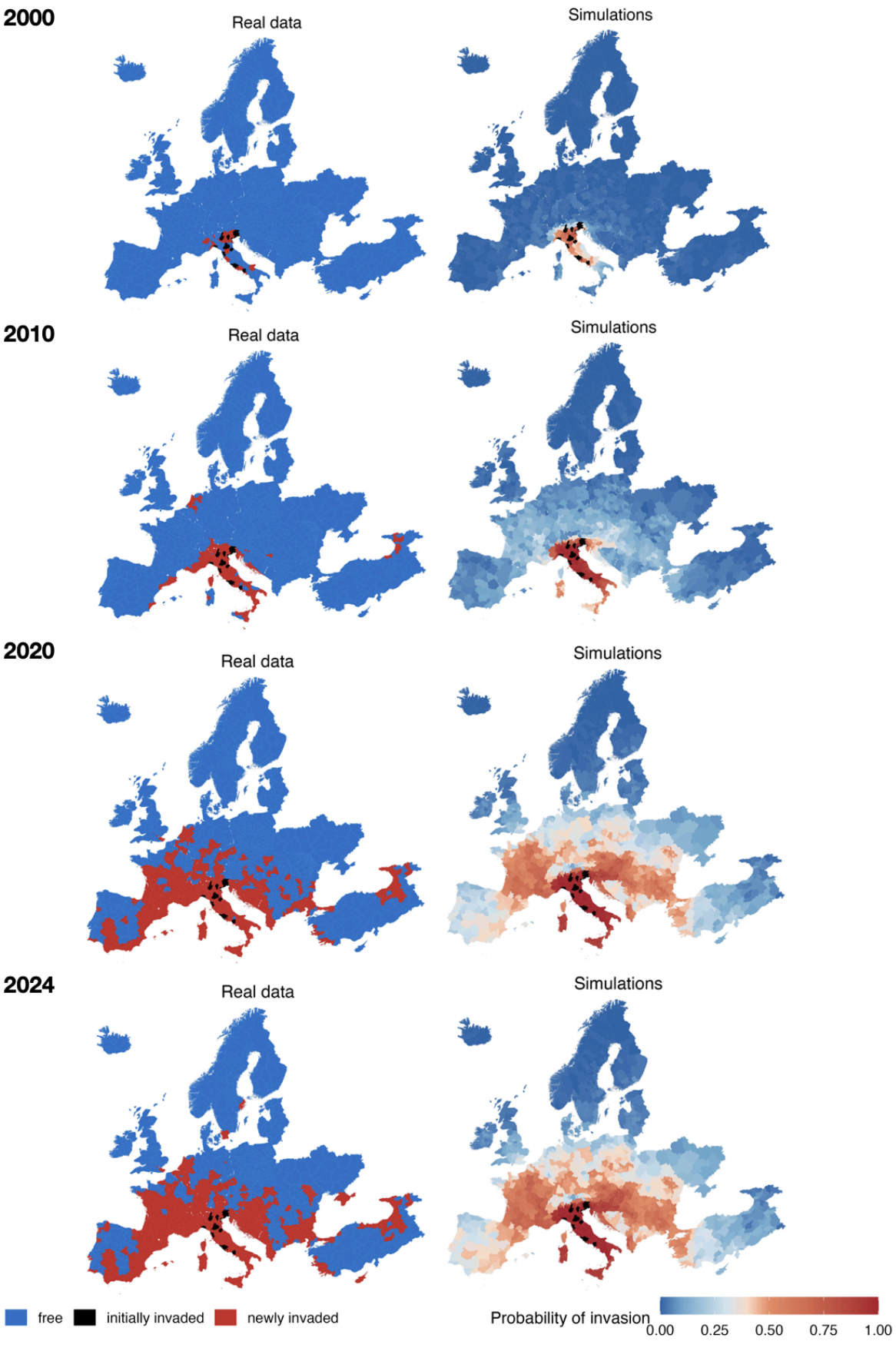
2000
Real data
Simulations
2010
Real data
Simulations
2020
Real data
Simulations
2024
Real data
Simulations
free
initially invaded
newly invaded
Probability of invasion
0.00
0.25
0.50
0.75
1.00

Figure 3. Spatiotemporal patterns of the past expansion of *Aedes albopictus* in Europe. For each year, observed invasion data are shown on the left, while the corresponding maps on the right display mean invasion probabilities derived from model simulations.

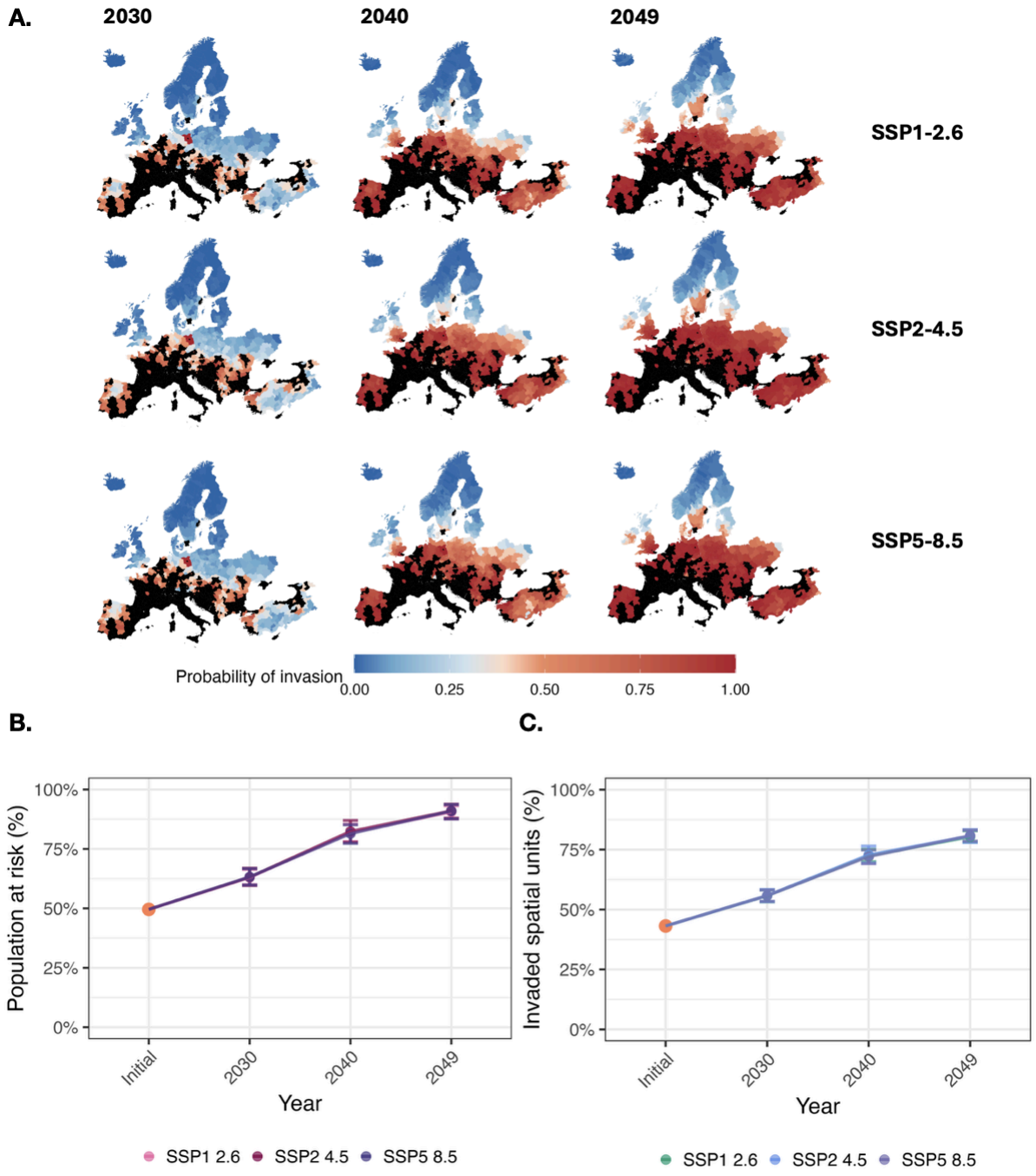

Figure 4. Predicted expansion of *Aedes albopictus* across Europe under three climate change scenarios (SSP1-2.6, SSP2-4.5 and SSP5-8.5). A. Maps representing the predicted probability of invasion by year for each scenario, aggregated across all model realizations. Black represents areas already invaded by the end of 2024. **B.** Increase in the proportion of the European population at risk (orange dot indicates the baseline proportion) for scenarios SSP1-2.6, SSP2-2.6 and SSP5-8.5 over time, aggregated across all model realizations. **C.** Increase in the proportion of invaded spatial units (orange dot indicates the baseline proportion) for scenarios SSP1-2.6, SSP2-2.6 and SSP5-8.5 over time, aggregated across all model realizations.